

01 Jan 1991

Occupation Dynamics of Trap States in an a-Si:H Thin-Film Transistor

J. N. Bullock

Cheng-Hsiao Wu

Missouri University of Science and Technology, chw@mst.edu

Follow this and additional works at: https://scholarsmine.mst.edu/ele_comeng_facwork



Part of the [Electrical and Computer Engineering Commons](#)

Recommended Citation

J. N. Bullock and C. Wu, "Occupation Dynamics of Trap States in an a-Si:H Thin-Film Transistor," *Journal of Applied Physics*, vol. 69, no. 2, pp. 1041-1046, American Institute of Physics (AIP), Jan 1991.

The definitive version is available at <https://doi.org/10.1063/1.347420>

This Article - Journal is brought to you for free and open access by Scholars' Mine. It has been accepted for inclusion in Electrical and Computer Engineering Faculty Research & Creative Works by an authorized administrator of Scholars' Mine. This work is protected by U. S. Copyright Law. Unauthorized use including reproduction for redistribution requires the permission of the copyright holder. For more information, please contact scholarsmine@mst.edu.

Occupation dynamics of trap states in an *a*-Si:H thin-film transistor

J. N. Bullock and C. H. Wu

Department of Electrical Engineering, University of Missouri-Rolla, Rolla, Missouri 65401

(Received 23 July 1990; accepted for publication 8 October 1990)

We calculate the dynamical behavior of *a*-Si:H thin-film transistors with an emphasis on the occupation dynamics of trap states. The appropriate rate equation for the occupation function of trap states is included. We show the relations of filling the trap states with the switch-on time and of emptying the trap charges with the switch-off time. The occupation functions in both cases are non-Fermi distribution. The quasi-equilibrium approximation underestimates those two time constants. Thus, transit time theory cannot describe the speeds of transistors made from disordered materials.

I. INTRODUCTION

In recent years, the hydrogenated amorphous silicon thin-film transistor (*a*-Si:H TFT) has emerged as the leading device for driving large-area active-matrix liquid-crystal displays.¹ In such a flat-panel display, each pixel has one *a*-Si:H TFT that serves as a switch the same way as a crystalline silicon field-effect transistor (FET) is used in a dynamic random-access-memory device in connecting to a storage capacitor. In a crystalline FET, the switch-on speed is directly related to the transit time from the source to the drain because the transit time is the figure of merit for establishing the conducting channel and hence the steady state of the device. However, in *a*-Si:H TFTs, there exists a large amount of continuous distributed trap states in the energy gap² and at equilibrium the Fermi level is about 0.5 eV or more below the conduction-band edge. Therefore, for every free carrier at a given position along the channel, there are at least ten more trapped charges at the same position. Within a transit time, the number of free carriers accumulated is so insufficient that the channel is only weakly formed. As we shall show, it takes much more time to firmly establish the conducting channel. This intuitively explains why a transit time is not the order-of-magnitude estimate for the time to reach steady state in *a*-Si:H TFTs.

In the case of switching off, time reversal holds for the crystalline FETs. However, in *a*-Si:H TFTs, the filling and emptying of trap states involve different physical parameters. Thus, the switch-on time depends on the filling rate of the trap states and the switch-off time depends on the emptying rate of the deepest trap states near the equilibrium Fermi level or the initial quasi-Fermi level. The emptying and filling of the trap states at all locations of the conducting channel are the central processes that determine the time to reach a steady state, and those occupation dynamics are the emphasis of our investigation.

The *a*-Si:H TFT has been studied by many investigators. Earlier efforts have been centered around the static characteristics of the device due to the effects of large bulk band-tail states and the importance of the semiconductor-insulator interface-state effect.³⁻¹⁴ Dynamic characteristics have been analyzed by Matsumura *et al.*^{15,16} for the "switch-off" case. However, their calculation is based on an inaccurate

quasi-thermal equilibrium approximation for the occupation of trap states, which can also be written as

$$f = \{1 + \exp[(\epsilon - qV + q\phi_n)/kT]\}^{-1}, \quad (1)$$

where V is the electric potential, ϕ_n the electron quasi-Fermi level, and ϵ is the energy of the trap state. This approximation assumes that occupation function f depends on time only implicitly through free-electron density (or quasi-Fermi level ϕ_n). As soon as the free-electron density changes, the corresponding Fermi distribution is reached immediately. As we will show in Sec. III, this underestimates the time required to build up or remove the trapped charge and hence their calculations reflect a much shortened time required to reach steady state.

The correct time evolution of the occupation function is determined by a Boltzmann equation or rate equation, where the "collision term" is replaced by the rates of moving "in" and "out" of a trap state, as shown by the general theory of Simmons and Taylor.¹⁷ This is discussed in Sec. II, where we present the model and the relevant equations. In Sec. III, we discuss our results by showing how the switch-on time relates to the filling of trap states and the switch-off time relates to the emptying of trap states. The occupation dynamics are the central part of such calculations and we present those correct results here for the first time.

II. PHYSICAL MODEL OF *a*-Si:H TFT

The device under investigation is an insulated-gate field-effect transistor (IGFET). The model is restricted to a single-gate device, although a similar model could be developed for a double-gate IGFET.⁶ The geometry of the device in our model is shown in Fig. 1. The semiconductor layer consists of *a*-Si:H which is assumed to be intrinsic or mildly *n* type with doping concentration N_D and the source and drain consist of a heavily doped *n*-type *a*-Si:H. Experimentally it has been observed that contacts of nearly all metals with *a*-Si:H are low resistance or ohmic,¹⁸ so the source and drain interfaces with the semiconductor are assumed to be ohmic.

The geometric parameters specified in the device model are the channel length L , the semiconductor layer thickness t_s , and the insulator thickness t_i . The material parameters are the semiconductor doping concentration N_D of the chan-

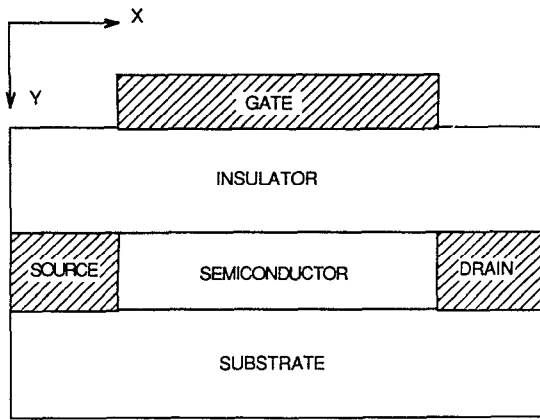


FIG. 1. Device geometry of *a*-Si:H thin-film transistor under consideration.

nel between the source and the drain, the insulator and semiconductor dielectric permittivity ϵ_i and ϵ_s , and the semiconductor's diffusivity D_n . The source contact (at $x = 0$) is taken to be at ground potential. When no voltage is applied to the gate, the energy bands are assumed to be flat. When a positive-gate voltage is applied, negative charges are pulled from the source and the drain and accumulated near the insulator-semiconductor interface when a conducting channel is formed. In our computational model, current is assumed to flow between the source and drain contacts (i.e., x direction) via majority carriers in the conduction channel. Thus the quasi-Fermi level in the y direction is assumed to be constant. In this approximation, only one-dimensional analysis of the current continuity equation is required.

The two-dimensional Poisson equation can be written as

$$\frac{\partial^2 \psi}{\partial x^2} + \frac{\partial^2 \psi}{\partial y^2} = -\frac{\rho}{\epsilon_s}, \quad (2)$$

where the space charge ρ is the sum of free electron n , ionized dopant N_D^+ , and trap charges from donorlike states $N_D(\epsilon)$ and acceptorlike states $N_A(\epsilon)$, so that

$$\rho = q \left(-n + N_D^+ + \int N_D(\epsilon) [1 - f(\epsilon)] d\epsilon - \int N_A(\epsilon) f(\epsilon) d\epsilon \right), \quad (3)$$

where $f(\epsilon, x, t)$ is the occupation function which is a function of gap state energy ϵ , position x , and time t and will be discussed later. The donorlike states can be approximated from experimental results as

$$N_D(\epsilon) = (N_v/kT) e^{(\epsilon_v - \epsilon)/\epsilon_D}, \quad (4)$$

and similarly

$$N_A(\epsilon) = (N_c/kT) e^{(\epsilon - \epsilon_c)/\epsilon_A}, \quad (5)$$

where $\epsilon_D = 43$ meV and $\epsilon_A = 27$ meV are used.¹⁹

In the very thin semiconductor layer limit, we assume that electric field varies linearly in the y direction so that

$$\begin{aligned} \frac{\partial^2 \psi}{\partial y^2} &= \frac{1}{t_s} \left(\frac{\partial \psi}{\partial y} \Big|_t - \frac{\partial \psi}{\partial y} \Big|_0 \right) \\ &= \frac{1}{t_s \epsilon_s} \left(\rho_{s1} + \rho_{s2} + \frac{\epsilon_i}{t_i} (\psi_G - \psi) \right), \end{aligned} \quad (6)$$

where ρ_{s1} and ρ_{s2} are two interface charges, ψ_G is the gate voltage, t_s is the semiconductor thickness, and t_i is the insulator thickness.

This implies that the charge distribution in the y direction is constant except possibly at the interfaces. In our model, there are no charges inside the insulator and the substrate layer is floating so that electric field inside is zero. Using the dimensionless unit of potential $V = q\psi/kT$, we reduce the Poisson equation to a one-dimensional (1D) equation, although it still retains the information from a two-dimensional (2D) model. Thus

$$\begin{aligned} \frac{\partial^2 V}{\partial x^2} &= \frac{q^2}{kT\epsilon_s} \left(N_c e^{V-E} - N_D^+ - \int [N_D(1-f) \right. \\ &\quad \left. + N_A f] d\eta + \frac{\epsilon_i}{\epsilon_s t_s t_i} (V - V_G) \right), \end{aligned} \quad (7)$$

where the free-electron density $n = N_c e^{V-E}$, E is the dimensionless quasi-Fermi level, and $\eta = q\epsilon/kT$ is the dimensionless energy. The interface charges ρ_{s1} and ρ_{s2} are neglected.

The dynamics of the occupation function for trap states f can be appropriately described by a rate equation based on Simmons and Taylor's theory for continuous distributions of trap states.¹⁷ The occupation of a particular trap level is controlled by two opposing processes of capture into the trap and emission into the conduction band. Thus

$$\frac{df}{dt} = \sigma v n (1-f) - e_n f, \quad (8)$$

where σ is the capture cross section, v is the thermal velocity, and e_n is the emission rate that is determined by the equilibrium condition so that

$$e_n = \sigma v N_c e^\eta. \quad (9)$$

Thus, Eq. (8) is simplified to

$$\frac{df}{dt} = \sigma v N_c e^{V-E} [1 - f(1 + e^{\eta - V + E})]. \quad (10)$$

We note that in the quasi-equilibrium approximation, the left-hand side of Eq. (10) is zero and f is then identical to Fermi distribution as given in Eq. (1).

If we consider *a*-Si:H TFT as a unipolar device so that generation and recombination effects can be neglected, then the time-dependent continuity equation can be written as

$$\frac{\partial \rho}{\partial t} + \frac{\partial J_n}{\partial x} = 0, \quad (11)$$

where the first term of Eq. (11) contains the displacement current through the Poisson equation and the total conduction current and the electron current, J_n , are identical and are given by

$$J_n = -q D_n n \frac{\partial E}{\partial x}. \quad (12)$$

The time derivative of space charge ρ in Eq. (11) can be obtained from Eq. (3) to yield the current continuity equa-

tion that is expressed in terms of variable E , the quasi-Fermi level, and can be written as

$$\begin{aligned} \frac{\partial^2 E}{\partial x^2} + \frac{\partial E}{\partial x} \left(\frac{\partial V}{\partial x} - \frac{\partial E}{\partial x} \right) \\ = -\frac{1}{D_n} \left(\frac{\partial V}{\partial t} - \frac{\partial E}{\partial t} + \sigma v \int (N_D + N_A) \right. \\ \left. [1 - f(1 + e^{\eta - \nu + E})] d\eta \right). \end{aligned} \quad (13)$$

The simultaneous solutions of three coupled equations of Eqs. (7), (10), and (13) for variables V , E , and f as function of position x and time t are evaluated numerically using implicit finite-difference equations for the second-order differential equations (7) and (13) and a single-step backward Euler method for the first-order differential equation (10) because the emission rate varies more than 20 orders of magnitude from top of the energy gap to the bottom. The occupation function is further transformed into an exponential variable and has a uniform mesh in energy while an adaptive nonuniform mesh in position is used for V and E .

III. RESULTS AND DISCUSSIONS

Equations (7), (10), and (13) are solved for V , f , and E at every point along the source-drain channel for a given time t using the following input parameters:

$$\begin{aligned} D_n = 0.33 \text{ cm}^2/\text{s}, \quad T = 300 \text{ K}, \quad N_D = 10^{12} \text{ cm}^{-3}, \\ t_s = 10^{-5} \text{ cm}, \quad t_i = 10^{-5} \text{ cm}, \quad L = 2 \times 10^{-4} \text{ cm}, \\ \epsilon_s = 11.0, \quad \text{and} \quad \epsilon_i = 3.9. \end{aligned}$$

In the first example, we show a case when both gate and drain-source voltage are turned on simultaneously from equilibrium condition. At turn-on voltages of $\psi_{DS} = 0.25 \text{ V}$ and $\psi_G = 0.5 \text{ V}$, the free-electron concentration is shown in Fig. 2 for successive intervals of time. At $t = 10^{-14} \text{ s}$ the concentration is almost uniform as in the case of equilibrium. In that interval, the Poisson equation resembles the La-

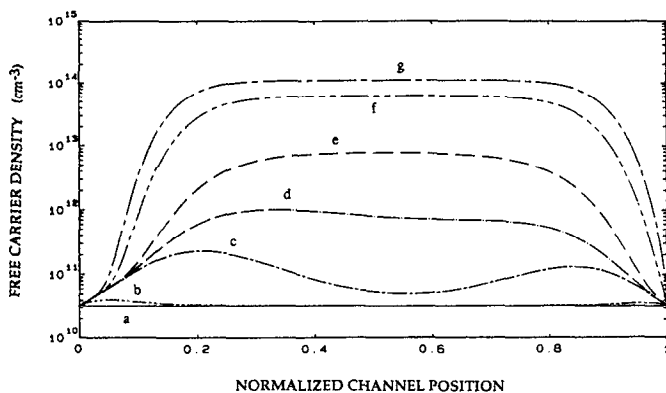


FIG. 2. Free-electron concentration vs distance for $\psi_{DS} = 0.25 \text{ V}$ and $\psi_G = 0.50 \text{ V}$. Each curve is for a different time: (a) 10^{-14} s , (b) 10^{-10} s , (c) 10^{-8} s , (d) 10^{-7} s , (e) 10^{-6} s , (f) 10^{-5} s , (g) 10^{-4} s to steady state.

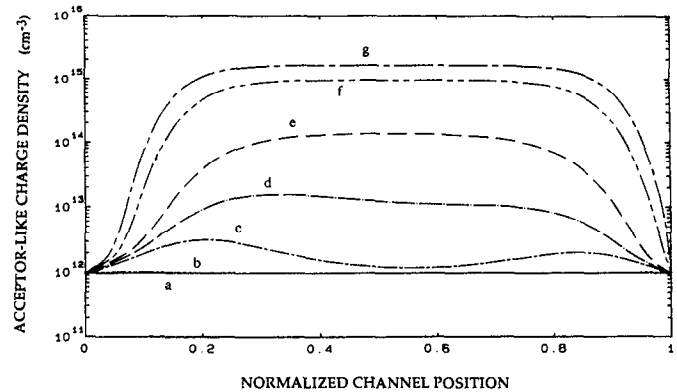


FIG. 3. Charged acceptorlike state concentration vs distance for $\psi_{DS} = 0.25 \text{ V}$ and $\psi_G = 0.50 \text{ V}$. Each curve is for a different time: (a) 10^{-14} s , (b) 10^{-10} s , (c) 10^{-8} s , (d) 10^{-7} s , (e) 10^{-6} s , (f) 10^{-5} s , (g) 10^{-4} s to steady state.

place equation because no appreciable space charge has flowed into the channel. However, at $t = 10^{-8} \text{ s}$ [curve (c)], which is the order of the transit time, the channel is only weakly formed, the two peaks in the curve show that electrons are pulled in from both the source and the drain contacts. This is still far from steady state. At $t = 10^{-7} \text{ s}$, a uniform channel exists except near the two boundaries. However, the free-carrier density is still two orders of magnitude below the steady-state value, which is reasonably reached at $t \geq 10^{-5} \text{ s}$ [curve (f)]. From 10^{-1} s on, the electron concentration is essentially unchanged. This is distinctly different from the time-dependent channel formation in crystalline FETs. In the switch-on of a -Si:H TFTs, the free-electron concentration will increase only in cooperation with filling of the trap states. This can be observed from the filling of the corresponding acceptorlike states as shown in Fig. 3. Note the similarity in the shape of each curve as compared to the corresponding free-electron curve in Fig. 2 except that the order of magnitude is one higher. The occupation function, $f(\epsilon, x, t)$, depends on gap state energy as well as position x in the channel. At $x = 0.23$, $f(\epsilon, t)$ is shown in Fig. 4 at various time intervals. At time $t = 10^{-14} \text{ s}$ [curve (a)], f is almost an equilibrium Fermi distribution. At steady state [curve (d)], the Fermi level, E_f , is shifted about 0.2 eV towards the conduction band. However, at the intermediate stage, a non-Fermi distribution is obtained. It is evident that at $t = 10^{-6} \text{ s}$ [curve (b)], the quasi-equilibrium approximation fails to obtain the correct result. If curve (b) is approximated by a Fermi distribution with a time-dependent E_f , the net effect is that higher-energy trap states are filled "completely" too quickly. Curve (b) clearly indicates "partially" filled higher-energy trap states. Thus, the quasi-equilibrium approximation grossly underestimates the time to reach steady state. In crystalline FETs, the time-dependent continuity equation (or dn/dt term) determines the switch-on time, which is the order of the transit time because of the drift-diffusion mechanism is described in the transport equa-

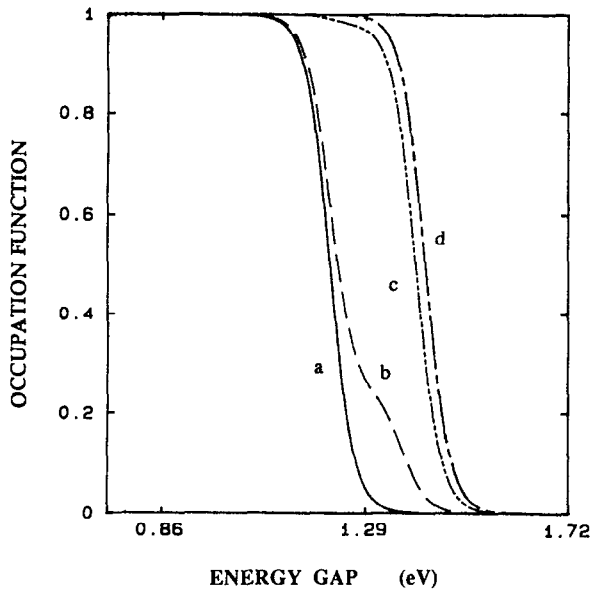


FIG. 4. Occupation function at $x = 0.23$ for $\psi_{DS} = 0.25$ V and $\psi_G = 0.50$ V. Each curve is for a different time: (a) 10^{-14} s (b) 10^{-6} s (c) 10^{-5} s (d) 10^{-3} s to steady state. Energy of 1.72 eV is located at the mobility edge of the conduction band.

tion. In the quasi-equilibrium approximation of Matsuura,¹⁶ the switch-on time is again determined by the continuity equation except that the dn/dt term is affected by the presence of a large amount of trapped charges included in the Poisson equation. Here, we show that the switch-on time is not determined by the dn/dt term, but rather by the df/dt term of Eq. (10), which is much larger than dn/dt term in the continuity equation [or equivalently, the last term on the right-hand side of Eq. (13), which is set to zero in the quasi-equilibrium approximation]. Thus, the switch-on time is the time of filling all the trap states from the equilibrium E_f up to the steady state E_f . A rough estimate can be made by using $df/dt \approx \sigma v n (1 - f)$. Since $\sigma v \approx 4 \times 10^{-8}$ cm³/s and n has

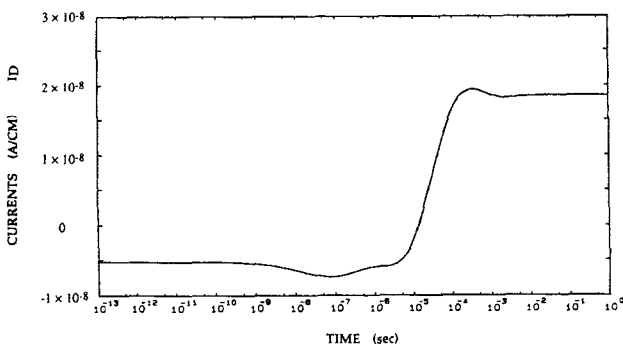


FIG. 5. Drain current I_D per unit channel width vs time for $\psi_{DS} = 0.25$ V and $\psi_G = 0.50$ V.

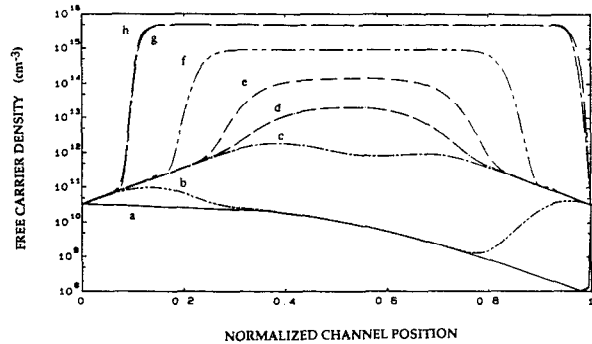


FIG. 6. Free-electron concentration vs distance for $\psi_{DS} = 2.5$ V and ψ_G turning on to 5.0 V. Each curve is for a different time: (a) 10^{-14} s, (b) 10^{-10} s, (c) 10^{-8} s, (d) 10^{-7} s, (e) 10^{-6} s, (f) 10^{-5} s, (g) 10^{-4} s, (h) 10^{-2} s to steady state.

the initial value about 10^{10} cm⁻³ and the final value of 10^{14} cm⁻³. Thus the switch-on time is somewhere between 2.5×10^{-3} to 2.5×10^{-7} s. Our calculation shows that the switch-on time is at least the order of 10^{-5} s as indicated by curve *f* in Fig. 2. A clearer picture of the switch-on time can be evaluated through the drain current, $I_D(t)$, which is shown in Fig. 5. Initially electrons are pulled from the drain contact into the channel, thus the current is negative. When finally electrons are flowing into the drain contact from the channel, the current is positive. Thus, at 10^{-3} s, I_D is more or less steady and this time can be considered as the switch-on time and we note that this is five orders of magnitude greater than the transit time. We also note that it is not necessary to calculate a case with a longer channel to prove this effect of occupation dynamics on switch-on time. When a longer channel is used, the flat region of the free-carrier concentration curve in Fig. 3 is extended.¹⁴

In the second example, we show a case where the gate voltage is turned on to 5.0 V after the drain-source voltage has been at 2.5 V for a long time. The voltage drop at any given position along the channel except near the boundaries is thus about 2.5 V from $t = 0^+$ to the steady state. The free-electron concentration along the channel is shown in Fig. 6. At $t = 10^{-14}$ s [curve (a)], the free-electron concentration is essentially at the equilibrium value where a dip at $x \approx 0.98$ indicates the initial condition of $\psi_{DS} = 2.5$ V so that there is a very small constant flow of electrons to the drain side. At $t = 10^{-10}$ s the two peaks of curve (b) near the source and the drain indicate that extra electrons are being drawn into the channel from the two terminals. At $t = 10^{-8}$ s [curve (c)], the order of a transit time, the two peaks are now merged. Yet this is far from the steady state since we indicated, as in the first example, that a large number of electrons is required to fill the trap states in order to fill the channel with enough free electrons. This is evident at $t = 10^{-4}$ s [curve (g)], where near steady state is reached. The free-electron concentration at steady state is at a constant 5×10^{15} /cm⁻³ except near the two terminals. Again, the filling of acceptor-

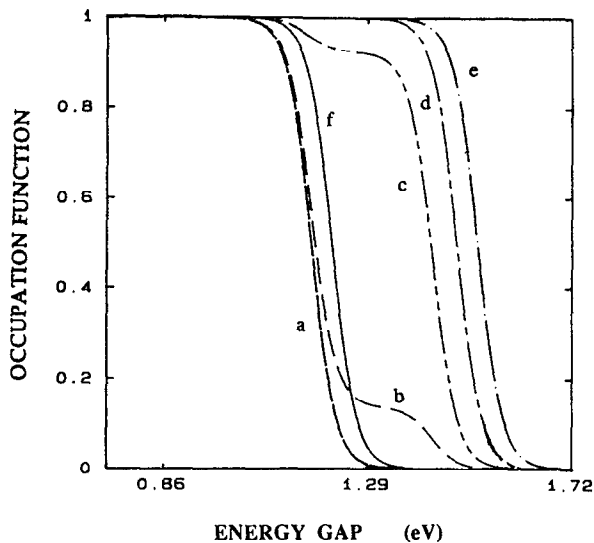


FIG. 7. Occupation function at $x = 0.5$ for $\psi_{DS} = 2.5$ V and ψ_G turning on to 5.0 V. Each curve is for a different time: (a) 10^{-14} s, (b) 10^{-7} s, (c) 10^{-6} s, (d) 10^{-5} s, (e) 10^{-4} s to steady state. (f) Equilibrium occupation function.

like trap states follows a similar trend as the buildup of free electrons except that the amount is one order of magnitude higher. The occupation functions at $x = 0.5$ and $x = 0.81$ along the channel are shown in Figs. 7 and 8 for various time intervals. In Fig. 7, curves (b) and (c) show the change of occupation function from $t = 10^{-7}$ s to $t = 10^{-6}$ s. This clearly shows how acceptorlike states are filled "gradually" in a totally non-Fermi-distribution-like manner. From

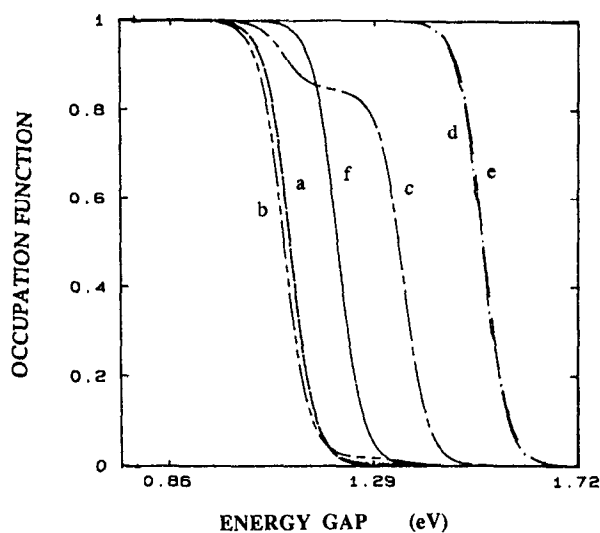


FIG. 8. Occupation function at $x = 0.81$ for $\psi_{DS} = 2.5$ V and ψ_G turning on to 5.0 V. Each curve is for a different time: (a) 10^{-14} s, (b) 10^{-6} s, (c) 10^{-5} s, (d) 10^{-4} s, (e) 10^{-1} s to steady state. (f) Equilibrium occupation function.

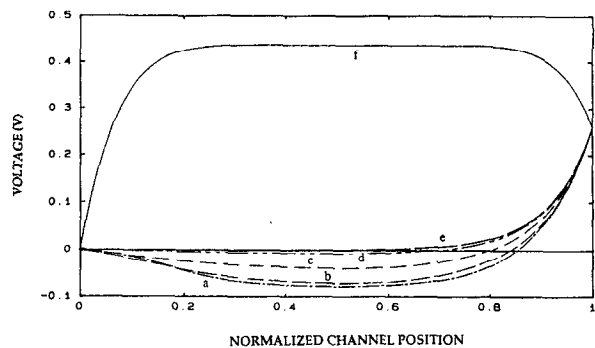


FIG. 9. Electrostatic potential vs distance for $\psi_{DS} = 0.25$ V and ψ_G turning off from 0.50 V to zero. (a) 10^{-14} s, (b) 10^{-8} s, (c) 10^{-7} s, (d) 10^{-6} s, (e) 10^{-5} s to steady state. (f) Voltage before gate was turned off.

$t = 10^{-5}$ s on, the occupation function is then closer to a Fermi distribution. Figure 8 is similar to Fig. 7, except that the shift of initial E_f to final E_f is larger. Again the gradual filling of trap states is the same as in Fig. 7. Note that, in the second example, we have considerably increased the applied voltages. The behavior of carrier concentrations and the occupation dynamics are similar to when the applied voltages are smaller, as indicated by the first example. Thus, it is not necessary to use high applied voltages to illustrate the simulated results.

In the third example, we show a case where initially both source-drain and gate voltages are on at $\psi_{DS} = 0.25$ V and $\psi_G = 0.5$ V, and then at $t = 0$ the gate is turned off. The electric potential at various time intervals is shown in Fig. 9. The gradients of the potential near the two terminals are of opposite sign, indicating the electric fields needed to remove free electrons out of both terminals. The free-electron concentration is shown in Fig. 10. The concentration from the

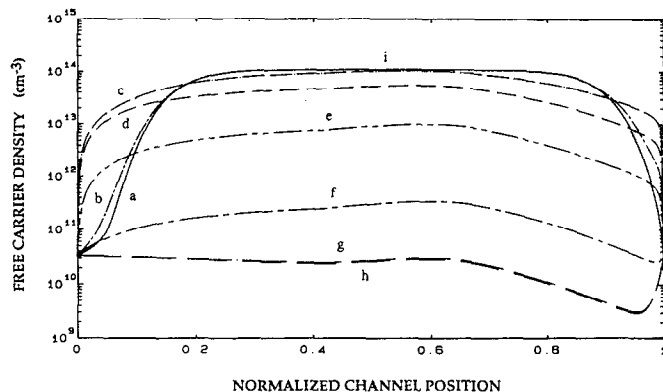


FIG. 10. Free-electron concentration vs distance for $\psi_{DS} = 0.25$ V and ψ_G turning off from 0.50 V to zero. Each curve is for a different time: (a) 10^{-14} s, (b) 10^{-10} s, (c) 10^{-8} s, (d) 10^{-7} s, (e) 10^{-6} s, (f) 10^{-5} s, (g) 10^{-4} s, (h) 10^{-1} s to steady state. (i) Free-carrier density before gate was turned off.

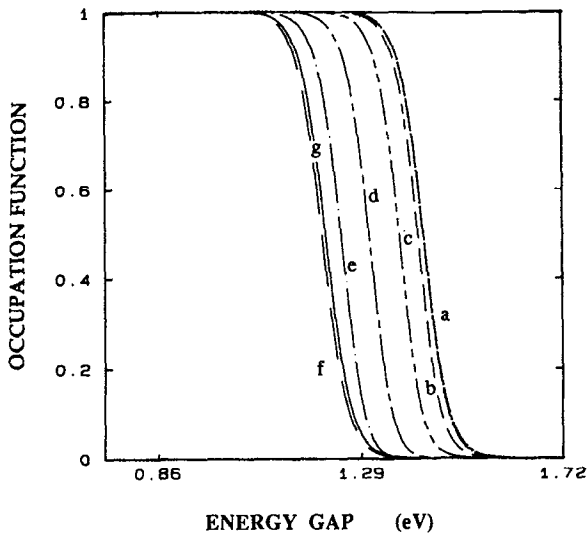


FIG. 11. Occupation function at $x = 0.5$ for $\psi_{DS} = 2.5$ V and ψ_G turning on to 5.0 V. Each curve is for a different time: (a) 10^{-14} s, (b) 10^{-7} s, (c) 10^{-6} s, (d) 10^{-5} s, (e) 10^{-4} s, (f) 10^{-1} s to steady state. (g) Equilibrium occupation function.

initial state up to $t = 10^{-14}$ s is shown in curve (a). At time $t = 10^{-8}$ s [curve (c)], the free electrons have dispersed to reach both terminals through both drift and diffusion mechanisms. From that time on, the channel is gradually emptying most of the free electrons as well as the trap charges. This is clear from the occupation function at $x = 0.5$ as shown in Fig. 11. Even in the case of emptying traps, the occupation function is not Fermi-distribution like as would be in the case of the quasi-equilibrium approximation. For example, curve (b) at $t = 10^{-7}$ s is not curve (a) by the Fermi-level shift. Because trap states at the higher-energy tail are depleted faster than the lower-energy states, the curve is "tilted up" a bit as compared to curve (a). The time required to empty the excess trapped charge is more than $t = 10^{-4}$ s as shown in curve (e). The "switch-off" time is generally different from the "switch-on" time in α -Si:H TFTs because the switch-on time depends on filling of the trap states while the switch-off time depends on emptying of the excess trap charges. This is evident by comparing the occupation function curves of Figs. 7 and 11. Clearly there is no time-reversal behavior between switch-on and switch-off. The filling and emptying of those trap states are contained in separate terms on the right-hand side of Eq. (8) (first term is filling, second term is emptying) and hence will have separate time constants. The deepest trap state to be emptied in our example is at $E_f = 1.2$ eV or about 0.5 V from the conduction-band edge. Thus we can estimate the switch-off time by using the relation

$$\frac{df}{dt} = -\sigma v N_c e^{-(E_c - E_f)/kT} f = -1.6 \times 10^3 f.$$

Thus, the time constant is of the order of 10^{-3} s. The E_f shift is approximately from $E_f = 1.42$ eV to $E_f = 1.20$ eV. Thus the sum of two terminal currents, I_D and I_S , will reflect the density of states at the energy which moves toward E_f with time. The transient currents collected can thus be used to probe the density of states at that small energy range.

IV. CONCLUSIONS

We present the correct system of equations to evaluate the dynamical characteristics of α -Si:H TFTs. We show that the filling and emptying of trap states determine the switch-on and switch-off time constants associated with the operation of the TFTs. The occupation functions are non-Fermi-distribution like in both cases. Those occupation dynamics of trap states are presented for the first time. By comparing those results using the quasi-equilibrium approximation with our accurate ones, it is found that a much longer time is required to reach steady state if the device is to switch on or to reach equilibrium state if the device is to switch off. In our examples, those time constants are of the order of 10^{-3} s, which are to be verified experimentally. Our calculations also show that the transit-time theory with the inclusion of a large amount of the trap states is incorrect in evaluating the on-off speeds of α -Si:H TFTs.

- ¹ R. K. Jorgen, IEEE Spectrum 26, 60 (1989).
- ² W. E. Spear and P. G. Lecomber, J. Non-Cryst. Solids 8-10, 727 (1972).
- ³ T. C. Luo, I. Chen, and R. C. Genovevse, IEEE Trans. Electron Devices ED-28, 740 (1981).
- ⁴ G. W. Neudeck and A. K. Malhotra, Solid-State Electron. 19, 721 (1976).
- ⁵ M. Shur and M. Hack, J. Non-Cryst. Solids 59-60, 1174 (1983).
- ⁶ I. Chen and T. C. Luo, J. Appl. Phys. 52, 3020 (1980).
- ⁷ I. Chen and F. C. Luo, Solid State Electron. 24, 257 (1980).
- ⁸ M. J. Powell, B. D. Easton, and O. T. Hill O, Appl. Phys. Lett. 38, 794 (1981).
- ⁹ S. Lee and I. Chen, Appl. Phys. Lett. 41, 558 (1982).
- ¹⁰ I. Chen and F. C. Luo, J. Appl. Phys. 52, 4 (1981).
- ¹¹ M. J. Powell and J. Pritchard, J. Appl. Phys. 54, 3244 (1983).
- ¹² I. Chen, J. Appl. Phys. 56, 2 (1984).
- ¹³ G. W. Neudeck, K. Y. Chung, and J. F. Bare, Solid State Electron. 29, 639 (1986).
- ¹⁴ M. L. De Wever, Thesis, University of Missouri-Rolla, 1989.
- ¹⁵ S. Kishida, Y. Narube, Y. Ushida, and Y. M. Matsumura, Jpn. J. Appl. Phys. 22, 511 (1983).
- ¹⁶ J. Yue, S. Oda, and M. Matsumura, Jpn. J. Appl. Phys. 27, L919 (1988).
- ¹⁷ J. G. Simmons and G. W. Taylor, Phys. Rev. B 4, 1541 (1971).
- ¹⁸ M. H. Cohen, H. Fritzsche, and S. R. Ovshinsky, Phys. Rev. Lett. 22, 1065 (1969).
- ¹⁹ T. Tiedje, J. M. Celbulka, D. L. Morel, and B. Abeles, Phys. Rev. Lett. 46, 1425 (1981).